



Offset-sparsity decomposition for enhancement of microscopic images of stained specimens in histopathology, [1]

Ivica Kopriva¹, Marijana Popović Hadžija¹, Mirko Hadžija¹, Gorana Aralica^{2,3}

¹Ruđer Bošković Institute

²Clinical Hospital Dubrava

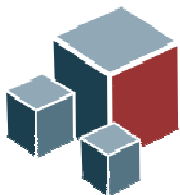
³School of Medicine, University of Zagreb

e-mail: ikopriva@irb.hr ikopriva@gmail.com

Web: <http://www.lair.irb.hr/ikopriva/>

September 22, 2015

Acknowledgment:



Croatian Science Foundation Grant 9.01/232 “Nonlinear component analysis with applications in chemometrics and pathology”.

1. I. Kopriva, M. Popović Hadžija, M. Hadžija, G. Aralica (2015). Offset-sparsity decomposition for automated enhancement of color microscopic image of stained specimen in histopathology, *Journal of Biomedical Optics* 20 (7), 076012 (July 28, 2015); doi: 10.1117/1.JBO.20.7.076012 (15 pages)



Rudjer Boskovich Institute, Zagreb, Croatia

<https://www.irb.hr/eng>

The Ruđer Bošković Institute is regarded as Croatia's leading scientific institute in the natural and biomedical sciences as well as marine and environmental research, owing to its size, scientific productivity, international reputation in research, and the quality of its scientific personnel and research facilities.

The Institute is the leading and internationally most competitive Croatian institute by virtue of its participation in international research projects, such as the IAEA and EC FP5-7 programs funded by the European Commission, NATO, NSF, SNSF, DAAD and other international scientific foundations.

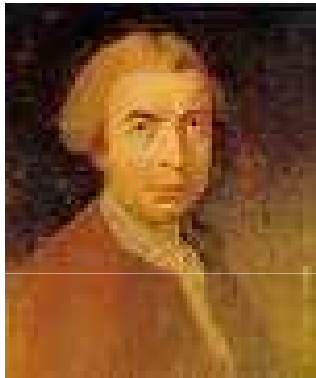
Today, the Ruđer Bošković Institute has over 550 scientists and researchers in more than 80 laboratories pursuing research in theoretical and experimental physics, physics and materials chemistry, electronics, physical chemistry, organic chemistry and biochemistry, molecular biology and medicine, the sea and the environment, informational and computer sciences, laser and nuclear research and development.





Roger Joseph Boskovich

http://en.wikipedia.org/wiki/Roger_Joseph_Boscovich



Rudjer Bošković (18 May 1711 – 13 February 1787) was a physicist, astronomer, mathematician, philosopher, diplomat, poet, theologian, Jesuit priest, and a polymath from the city of Dubrovnik in the Republic of Ragusa (today Croatia), who studied and lived in Italy and France where he also published many of his works.

Among his many achievements he was ***the first*** to suggest least absolute deviation based regression (1757). That was studied by Laplace (1793) and predated the least square technique originally developed by Legendre (1805) and Gauss (1823):

P. Bloomfield and W. L. Steiger. *Least Absolute Deviations: Theory, Applications, and Algorithms*. Birkhauser, Boston, MA, 1983.



Motivation

Visualization of different tissue structures in a histological specimen and the corresponding microscopic analysis undertaken by pathologists is still a basic clinical workflow required for an assessment of specimens and for diagnosing a disease. That is, pathologists look for visual cues to distinguish between healthy and diseased tissue. In this regard, various stains and tags are attached to biological tissues to improve the colorimetric difference between the tissue components (histological structures), thereby improving their visibility, [2,3].

However, due to the variations in the tissue preparation processes such as collection, preservation, sectioning, staining, and illumination, the tissue color and texture can vary considerably between specimens. These nonbiological experimental variations are also known as batch effects, [4,5].

2. J. M. Crawford, and A. D. Burt, "Anatomy, pathophysiology and basic mechanism of disease," in *Pathology of the Liver*, Sixth Edition, A. D. Burt, B. C. Portmann, and L. D. Ferrell, Eds., pp. 1-77, Elsevier, Churchill Livingstone (2011).
3. P. A. Bautista, and Y. Yagi, "Digital simulation of staining in histopathology multispectral images: enhancement and linear transformation of spectral transmittance," *J. Biomed. Opt.* 17(5), 056013 (2012).
4. S. Kothari, et al., "Removing batch effects from histopathological images for enhanced cancer diagnosis," *IEEE J. Biomed. Health Inf.* 18(3), 765-772 (2014).
5. J. H. Phan, C. F. Quo, C. Cheng, and M. D. Wang, "Multiscale integration of -omic, imaging, and clinical data in biomedical informatics," *IEEE Rev. Biomed. Eng.* 5, 75-87 (2012).



Motivation

For example, variation in the spectral signature of the stained tissue creates noise at image acquisition; this noise is also known as biochemical noise, [6,7].

These variations can change the quantitative morphological image features, and this makes it difficult to reach an accurate diagnosis, [4] e.g.in the field of digital pathology, i.e. computerized image analysis, [8].

Furthermore, as shown in a recent study, [9], pathology experts are sensitive to color variations.

Outlined problems related to the variations in the quality of the staining process were the motivation for the development of an automated image enhancement method, particularly for enhancing the colorimetric difference between the histological structures present in the images of a stained specimen.

6. K. R. Castleman, et al., "Classification accuracy in multiple color fluorescence imaging microscopy," *Cytometry* 41(2), 139-147 (2000).

7. M. Gavrilovic, et al., "Blind color decomposition of histological images," *IEEE Trans. Med. Imag.* 32(6), 983-994 (2013).

8. A. J. Mendez, et al., "Computer-aided diagnosis: Automatic detection of malignant masses in digitized mammograms," *Med. Phys.* 25, 957-964 (1998).

9. Lj. Platiša, et al., "Psycho-visual evaluation of image quality attributes in digital pathology slides viewed on a medical color LCD display," *Proc. SPIE* 8676, 86760J (2013).



Motivation

To be practically relevant, a method is required to be truly unsupervised, i.e., not to require any prior information from the user and be completely data driven.

A method would also need to demonstrate the validity and robustness of performance on images of different tissues stained, possibly, by various stains.

Hence, an automated image enhancement method is proposed in [1]. It is based on the decomposition of an unfolded color image of a stained specimen into **a sum** of the **approximately constant offset matrix** and the **sparse matrix**, which **denotes an improved image** with an enhanced colorimetric difference between histological structures.

The proposed method can be seen as a special (degenerative) case of the **rank-sparsity decomposition** (RSD) that decomposes a matrix into a sum of low-rank and sparse matrices, [10,11].

1.I. Kopriva, M. Popović Hadžija, M. Hadžija, G. Aralica (2015). Offset-sparsity decomposition for automated enhancement of color microscopic image of stained specimen in histopathology, *Journal of Biomedical Optics* 20 (7), 076012 (July 28, 2015); doi: 10.1117/1.JBO.20.7.076012 (15 pages) .

10. E. J. Candès, X. Li, Y. Ma, and H. Wright, "Robust principal component analysis?," *J. ACM* 58, 11 (2011).

11. V. Chandrasekaran, S. Sanghavi, P. A. Parrilo, and A. S. Willsky, "Rank-sparsity incoherence for matrix decomposition," *SIAM J. Opt.* 21, 572-596 (2011).



Offset-sparsity decomposition

The method proposed herein decomposes vectorized spectral images into a **sum** of an **approximately constant offset vector** and a **sparse vector**. We name the method OSD.

The offset term corresponds to the L_2 -norm-based regularization, and the sparse term corresponds to the L_1 -norm-based regularization in an optimization problem related to the minimization of the difference between the vectorized spectral images and the model.

Since the proposed method is similar to RSD, the accelerated proximal gradient method, [12-15] used for solving the RSD problem can be used for OSD as well.

12. Z. Lin, et al., "Fast convex optimization algorithms for exact recovery of a corrupted low-rank matrix," *UIUC Technical Report UILU-ENG-09-2214* (2009).
13. A. Beck, and M. Teboulle, "A fast iterative shrinkage-thresholding algorithm for linear inverse problems," *SIAM J. Image. Sci.* 2(1), 183-202 (2009).
14. K. C. Toh, and S. Yun, "An accelerated proximal gradient algorithm for nuclear norm regularized least square problems," *Pac. J. Opt.* 6(3), 615-640 (2010).
15. M. Fukushima, and H. Mine, "A generalized proximal point algorithm for certain non-convex minimization problems," *Int. J. Sys. Sci.* 12(8), 989-1000 (1981).



Related work: sparseness constrained denoising in wavelet domain

Let us denote 3D RGB image as a tensor $\underline{\mathbf{X}} \in \mathbb{R}_{0+}^{I_1 \times I_2 \times 3}$ consisting of 3 spectral images corresponding with red, green and blue colors, where each image has size of $I_1 \times I_2$ pixels. An upper-case bold letter, e.g., \mathbf{X} , denotes a matrix; a lower-case bold letter, e.g., \mathbf{x} , denotes a vector; and an italicized lower-case letter, e.g., x , denotes a scalar. The random variable e that follows the Gaussian distribution with zero mean and variance σ^2 is denoted as $e \sim N(0, \sigma^2)$.

The standard model of the observed image assumed by many image denoising methods is as follows [16-19]:

$$\mathbf{b}_n = \mathbf{s}_n + \mathbf{e}_n \quad n \in \{1, 2, 3\}$$

where \mathbf{b}_n stands for intensity of observed image, \mathbf{s}_n stands for noiseless image and \mathbf{e}_n stands for AWGN.

16. D. Donoho, "De-noising by soft-thresholding," *IEEE Trans. Inf. Theory* 41(3), 613-627 (1995).

17. I. Daubechies, M. Defrise, and C. De Mol, "An iterative thresholding algorithm for linear inverse problems with a sparisty constraint," *Comm. Pure Appl. Math.* 57, 1413-1457 (2004).

18. F. Luisier, T. Blu, and M. Unser, "A new sure approach to image denoising: Interscale orthonormal wavelet thresholding," *IEEE Trans. Image Process.* 16(3), 593-606 (2007).

19. J. Portilla, V. Strela, M. J. Wainwright, and E. P. Simoncelli, "Image denoising using scale mixtures of Gaussians in the wavelet domain," *IEEE Trans. Image Process.* 12(11), 1338-1351 (2003).



Related work: sparseness constrained denoising in wavelet domain

Under AWGN assumption an optimal estimate of \mathbf{s}_n is obtained by solving the log-likelihood problem that is regularized by the addition of a wavelet-domain L_1 -penalty (a.k.a. sparseness constraint):

$$\min_{\mathbf{c}_{s_n}} \left\{ \left\| \mathbf{c}_{b_n} - \mathbf{c}_{s_n} \right\|_2^2 + \lambda \left\| \mathbf{c}_{s_n} \right\|_1 \right\}$$

where \mathbf{c}_{b_n} and \mathbf{c}_{s_n} denote the vectors of coefficients in a wavelet basis. The exact solution is obtained by soft-thresholding [16,17,20]:

$$\mathbf{c}_{s_n} = S_{\lambda/2}(\mathbf{c}_{b_n}) = \max(\mathbf{c}_{b_n} - \lambda/2, 0)$$

An estimate of \mathbf{s}_n is obtained through the inverse wavelet transform \mathbf{D} : $\hat{\mathbf{s}}_n = \mathbf{D}\mathbf{c}_{s_n}$. The threshold has been estimated adaptively by using the MATLAB function *thselect* with an option for Stein's unbiased risk estimator (SURE), [21, 22].

20. A. Chambolle, et al., "Nonlinear wavelet image processing: Variational problems, compression, and noise removal through wavelet shrinkage," *IEEE Trans Image Process.* 7(3), 319-335 (1998).

21. C. Stein, "Estimation of the mean of multivariate normal distribution," *Annals of Statistics* 9, 1135-1151 (1981).

22. D. L. Donoho, and I. M. Johnstone, "Adapting to unknown smoothness via wavelet shrinkage," *J. Am. Stat. Assoc.* 90, 1200-1224 (1995).



Related work: the retinex theory

The retinex methodology, [23-25], assumes that an observed image is a multiplication of the illumination and reflection intensity terms, whereas the **reflection term** represents an **enhanced image**. Therefore, the retinex method is applied to the value V channel in the HSV color space as follows:

$$\mathbf{v}(i_1, i_2) = \mathbf{i}(i_1, i_2)\mathbf{r}(i_1, i_2)$$

where (i_1, i_2) denotes the pixel location; \mathbf{i} , the illumination ("shadow") term; and \mathbf{r} , the reflection term that is of actual interest. By taking logarithm, etc., we can obtain an additive impact of the illumination as follows:

$$\mathbf{v}_{\log}(i_1, i_2) = \mathbf{i}_{\log}(i_1, i_2) + \mathbf{r}_{\log}(i_1, i_2)$$

\mathbf{r}_{\log} is then estimated as a solution of the optimization problem [23]:

23. D. Zosso, G. Tran, and S. Osher, "Non-local Retinex - A Unifying Framework and Beyond," *SIAM J. Imag. Sci.* 8(2), 787-826 (2015).

24. D. Zosso, G. Tran, and S. Osher, "A unifying retinex model based on non-local differential operators," *Proc. SPIE* 8657, 865702 (2013).

25. W. Ma, J.-M. Morel, S. Osher, and A. Chien, "An L1-based variational model for retinex theory and its application to medical images," in *Proc. IEEE Conf. Comp. Vis. Patt. Rec.*, pp. 153-160, (2011).



Related work: the retinex theory

$$\hat{\mathbf{r}}_{\log} = \min_{\mathbf{r}_{\log}} \left\{ \left\| \nabla_w \mathbf{r}_{\log} - \nabla_{w,f} \mathbf{i}_{\log} \right\|_1 + \alpha \left\| \mathbf{r}_{\log} \right\|_2 + \beta \left\| \mathbf{r}_{\log} - \mathbf{i}_{\log} \right\|_2 \right\}$$

where $\nabla_w \mathbf{r}_{\log}$ stands for the nonlocal gradient of \mathbf{r}_{\log} , see also Definition 3.7 in Ref. 23, and $\nabla_{w,f} \mathbf{i}_{\log}$ stands for the nonlocal filtered gradient of \mathbf{i}_{\log} , see also Definition 3.12 in Ref. 23.

As proposed in Ref. 23, in an example related to shadow removal from an image of a natural scene, we select $\alpha = \beta = 0.5$ and a hard thresholding filter \mathbf{f} with a threshold set to 0.015. Then, \mathbf{r} is estimated as $\hat{\mathbf{r}} = imadjust\left(\exp(\hat{\mathbf{r}}_{\log}) / \max(\exp(\hat{\mathbf{r}}_{\log}))\right)$, [23, 26], where *imadjust* represents a MATLAB image enhancement command.

A retinex-enhanced color image is obtained by transforming the enhanced value channel component image from the HSV back to the RGB color space.

26. MATLAB code for the non-local retinex algorithm [Online].

Available: <http://www.mathworks.com/matlabcentral/fileexchange/47562-non-local-retinex>. Last date of access: January 21, 2015.



Related work: rank-sparsity decomposition [10, 11]

Rank-sparsity decomposition (RSD), a.k.a. Robust PCA, relates to additive decomposition of a matrix \mathbf{B} into sum of low-rank matrix \mathbf{A} and sparse matrix \mathbf{S} : $\mathbf{B}=\mathbf{A}+\mathbf{S}$.

$$(\hat{\mathbf{A}}, \hat{\mathbf{S}}) = \min_{(\mathbf{A}, \mathbf{S})} \left\{ \frac{1}{2} \|\mathbf{B} - \mathbf{A} - \mathbf{S}\|_F^2 + \mu \|\mathbf{A}\|_* + \mu \lambda \|\mathbf{S}\|_1 \right\}$$

$\|\mathbf{A}\|_*$ denotes nuclear norm (sum of singular values) that is used as **convex relaxation** of **NP-hard rank-minimization** problem [14].

Above optimization problem admits unique solution with the value of the regularization parameter set to: $\lambda = 1/\sqrt{\max(I_1, I_2)}$. The fast proximal gradient (FPG) is used to solve related optimization problem [12].

Let us denote $\mathbf{X} = (\mathbf{A}, \mathbf{S})$, $g(\mathbf{X}) = \|\mathbf{A}\|_* + \lambda \|\mathbf{S}\|_1$, $f(\mathbf{X}) = \frac{1}{2} \|\mathbf{B} - \mathbf{A} - \mathbf{S}\|_F^2$.

10. E. J. Candès, X. Li, Y. Ma, and H. Wright, "Robust principal component analysis?," *J. ACM* 58, 11 (2011).

11. V. Chandrasekaran, S. Sanghavi, P. A. Parrilo, and A. S. Willsky, "Rank-sparsity incoherence for matrix decomposition," *SIAM J. Opt.* 21, 572-596 (2011).



Related work: rank-sparsity decomposition

Previous optimization problem can be formulated as:

$$\hat{\mathbf{X}} = \min_{\mathbf{X}} F(\mathbf{X}) \doteq f(\mathbf{X}) + \mu g(\mathbf{X})$$

A computationally efficient solution of this optimization problem is obtained by FPG by minimizing sequence of quadratic approximations to $F(\mathbf{X})$, denoted as $Q(\mathbf{X})$, and formed at specially chosen points \mathbf{Y} for Lipschitz constant $L > 0$:

$$Q(\mathbf{X}, \mathbf{Y}) \doteq f(\mathbf{Y}) + \langle \nabla f(\mathbf{Y}), \mathbf{X} - \mathbf{Y} \rangle + \frac{L}{2} \|\mathbf{X} - \mathbf{Y}\|_F^2 + \mu g(\mathbf{X})$$

By defining $h(\mathbf{Y}) \doteq \mathbf{Y} - \frac{1}{L} \nabla f(\mathbf{Y})$ we have:

$$\arg \min_{\mathbf{X}} Q(\mathbf{X}, \mathbf{Y}) = \arg \min_{\mathbf{X}} \left\{ \mu g(\mathbf{X}) + \frac{L}{2} \|\mathbf{X} - h(\mathbf{Y})\|_F^2 \right\}$$



Related work: rank-sparsity decomposition

By setting $\mathbf{Y}_k = \mathbf{X}_k + \frac{t_{k-1}-1}{t_k}(\mathbf{X}_k - \mathbf{X}_{k-1})$, where k denotes iteration indeks, for a sequence

$t_k = (1 + \sqrt{1 + 4t_{k-1}^2})/2$ the **convergence** of previous optimization problem is made **quadratic** [13, 27].

When $g(\mathbf{X}) = \lambda \|\mathbf{S}\|_1$, optimization problem has closed form solution: $\mathbf{S}_{k+1} = S_{\frac{\lambda \mu}{L}}(h(\mathbf{Y}_k^S))$.

When $g(\mathbf{X}) = \|\mathbf{A}\|_*$ optimization problem has closed form solution: $\mathbf{A}_{k+1} = \mathbf{U} \Sigma_{\mu/L}(\Sigma) \mathbf{V}^T$, where $\mathbf{U} \Sigma \mathbf{V}^T$ stands for the SVD of $h(\mathbf{Y}_k^A)$.

The most often suggested application of RSD is related to the **detection of rare events** from **surveillance videos** [10,28]. Therefore, the background is contained in a low-rank matrix and the foreground (which accounts for rare events) is held in a sparse matrix. Another often suggested application of RSD is related to the **removal of shadows and specularities** from face images, [10], thus increasing the accuracy of face recognition

27. Y. Nesterov, "A method of solving a convex programming problem with convergence rate $O(1/k^2)$," Soviet Math. Doklady. 27, 372-376 (1983).

28. N. S. Aybat, D. Goldfarb, and S. Ma, "Efficient algorithms for robust and stable principal component pursuit problems," *Comput. Optim. Appl.* 58(1), 1-29 (2014).



Offset-sparsity decomposition

In [1] we have proposed to solve the following optimization problem for vectorized spectral images \mathbf{b}_n , $n \in \{R, G, B\}$.

$$(\hat{\mathbf{a}}_n, \hat{\mathbf{s}}_n) = \min_{(\mathbf{a}_n, \mathbf{s}_n)} \left\{ \frac{1}{2} \|\mathbf{b}_n - \mathbf{a}_n - \mathbf{s}_n\|_2^2 + \mu \|\mathbf{a}_n\|_2 + \mu\lambda \|\mathbf{s}_n\|_1 \right\}$$

For a vector $\|\mathbf{a}_n\|_2 = \|\mathbf{a}_n\|_*$ the minimization of nuclear norm is reduced to minimization of L_2 -norm of a vector. For $g(\mathbf{x}) = \|\mathbf{a}_n\|_2$ optimization problem has closed form solution:

$$\mathbf{a}_{n(k+1)} = \mathbf{u} S_{\mu/L}(\sigma) \mathbf{v}^T, \text{ where } \mathbf{u} \sigma \mathbf{v}^T \text{ is the SVD of } h(\mathbf{y}_k^{\mathbf{a}_n}).$$

However, in the case of a vector, the SVD is trivial to compute. For a row vector $h(\mathbf{y}_k^{\mathbf{a}_n})$, $\mathbf{u} = \mathbf{1}$, $\sigma = \|h(\mathbf{y}_k^{\mathbf{a}_n})\|_2$, and $\mathbf{v}^T = h(\mathbf{y}_k^{\mathbf{a}_n}) / \|h(\mathbf{y}_k^{\mathbf{a}_n})\|_2$. Thus, closed-form solution related to minimization of $\|\mathbf{a}_n\|_2$ is:

$$\mathbf{a}_{n(k+1)} = S_{\mu/L} \left(\|h(\mathbf{y}_k^{\mathbf{a}_n})\|_2 \right) h(\mathbf{y}_k^{\mathbf{a}_n}) / \|h(\mathbf{y}_k^{\mathbf{a}_n})\|_2$$



Offset-sparsity decomposition

The closed-form solution related to $g(\mathbf{x}) = \lambda \|\mathbf{s}_n\|_1$ is standard soft-thresholding solution of the L_1 -norm regularized least square problem [16, 17]:

$$\mathbf{s}_{n(k+1)} = \mathcal{S}_{\frac{\lambda\mu}{L}} \left(h(\mathbf{y}_k^{\mathbf{s}_n}) \right)$$

The OSD FPG algorithm can be found in [1]. Application of OSD FPG method to enhancement of the RGB microscopic image is outlined below:

Inputs: $\mathbf{B} \in \mathbb{R}_{0+}^{3 \times I_1 I_2}$ unfolded RGB image of the stained specimen with vectorized grayscale images $\{\mathbf{b}_n \in \mathbb{R}_{0+}^{1 \times I_1 I_2}\}_{n=1}^3$ with the size $I_1 \times I_2$ pixels. Sparseness regularization constant $\lambda = 1/\sqrt{I_1 \times I_2}$. Threshold constant $\mu = 10^{-3}$. Lipschitz constant $L = 2$.

For $n=1:3$

$(\mathbf{a}_n, \mathbf{s}_n) = \text{OSD_FPG}(\mathbf{b}_n, \lambda, \mu, L)$

End



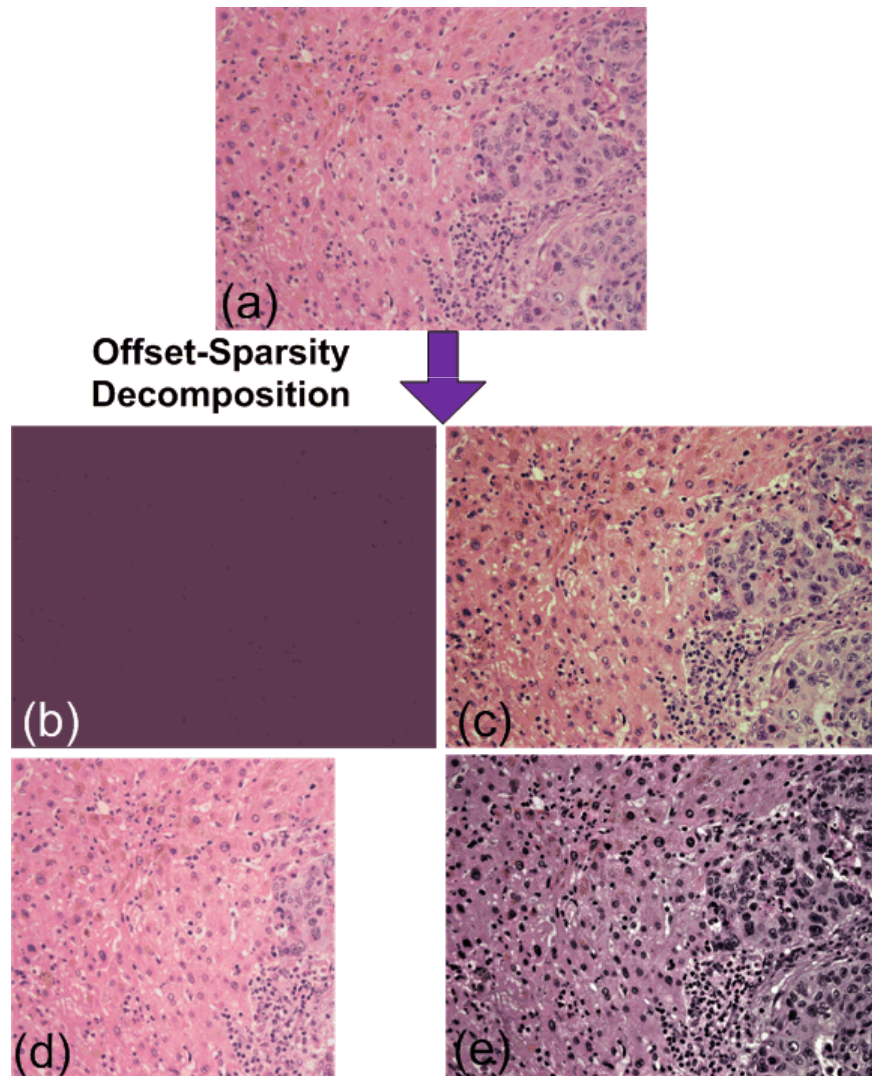
Offset-sparsity decomposition

$$\text{Set: } \mathbf{A} = \begin{bmatrix} \mathbf{a}_1 \\ \mathbf{a}_2 \\ \mathbf{a}_3 \end{bmatrix}, \mathbf{S} = \begin{bmatrix} \mathbf{s}_1 \\ \mathbf{s}_2 \\ \mathbf{s}_3 \end{bmatrix}.$$

Output: $\mathbf{S} \in \mathbb{R}_{0+}^{3 \times I_1 I_2}$ unfolded enhance color image of stained specimen. $\mathbf{A} \in \mathbb{R}^{3 \times I_1 I_2}$
unfolded image with the color offset term. The enhanced color image is obtained by
tensorizing \mathbf{S} : $\underline{\mathbf{S}} \in \mathbb{R}_{0+}^{I_1 \times I_2 \times 3}$.

MATLAB implementation of the OSD FPG algorithm with data used in [1] are available
at: <http://www.lair.irb.hr/ikopriva/publications.html>.

Offset-sparsity decomposition



Flow-chart diagram of the OSD method.

(a) H&E stained specimen of human liver with metastasis from colon cancer: MOS = 4.2, colorfulness = 0.446, sharpness = 9.38, contrast = 1.77. (b) **Color offset** term obtained by **OSD** algorithm. (c) **Image enhanced** with **OSD** algorithm: **MOS = 5, colorfulness = 0.619**, sharpness = 9.42, contrast = 1.57. (d) image enhanced with the **WT-ST-SURE** algorithm: MOS=3.8, colorfulness=0.443, sharpness=7.08, **contrast=1.87**. (e) image enhanced with the **L¹-Retinex** algorithm: MOS=2.8, colorfulness=0.305, **sharpness=13.75**, contrast=1.05.



Offset-sparsity decomposition

Image quality attributes:

colorfulness, [29], measures the amount of chrominance information that humans perceive. This attribute plays an important role in the quality of the color image of the stained specimen. It is estimated directly from the image according to:

$$colorfulness = 0.02 \times \log \left(\frac{\sigma_{\alpha}^2}{|\mu_{\alpha}|^{0.2}} \right) \times \log \left(\frac{\sigma_{\beta}^2}{|\mu_{\beta}|^{0.2}} \right)$$

where α = Red - Green color images; β = $0.5 \times (\text{Red} + \text{Green})$ - Blue color images; σ_{α}^2 , σ_{β}^2 , μ_{α} and μ_{β} represent the variance and mean along the α and β opponent color axes, respectively.



Offset-sparsity decomposition

sharpness, [29], is the attribute related to the preservation of fine details (edges) in a color image.

As described in [29], the Sobel edge detector is applied to each RGB color component. Then, binary edge maps are multiplied with the original values to obtain three grayscale edge maps. These grayscale edge maps are used for measuring the Weber contrast in a small window (3×3 pixels in the case of this study):

$$EME_{sharpness} = \frac{2}{k_1 k_2} \sum_{i=1}^{k_1} \sum_{j=1}^{k_2} \log \left(\frac{I_{\max,i,j}}{I_{\min,i,j}} \right)$$

where k_1 and k_2 denote the number of blocks across image dimensions, and $I_{\max,i,j}$ and $I_{\min,i,j}$ represent the maximal and minimal intensity value in each window, respectively. The sharpness measure for the color image is then estimated as [29]:

$$sharpness = \sum_{c=1}^3 \lambda_c EME_{sharpness} (grayedge_c)$$

where the weighting coefficients for the red, green, and blue components are as follows: $\lambda_1 = 0.299$, $\lambda_2 = 0.587$, and $\lambda_3 = 0.114$.



Offset-sparsity decomposition

contrast, [29], is defined as the ratio of the maximum and the minimum intensity of the entire image. Therefore, for a color image, it is calculated on the luminance component L^* in the CIE $L^*a^*b^*$ color space.

mean opinion score (MOS). We have asked five independent pathologists to evaluate the images of routinely stained specimens as well as the enhanced images. The images were graded on the scale from 1 to 5. Grade 5 refers to quality that yields the best perception of details in histological structures. This enabled us to obtain the mean opinion score (MOS) quality measure for images of stained specimens as well as for enhanced images.

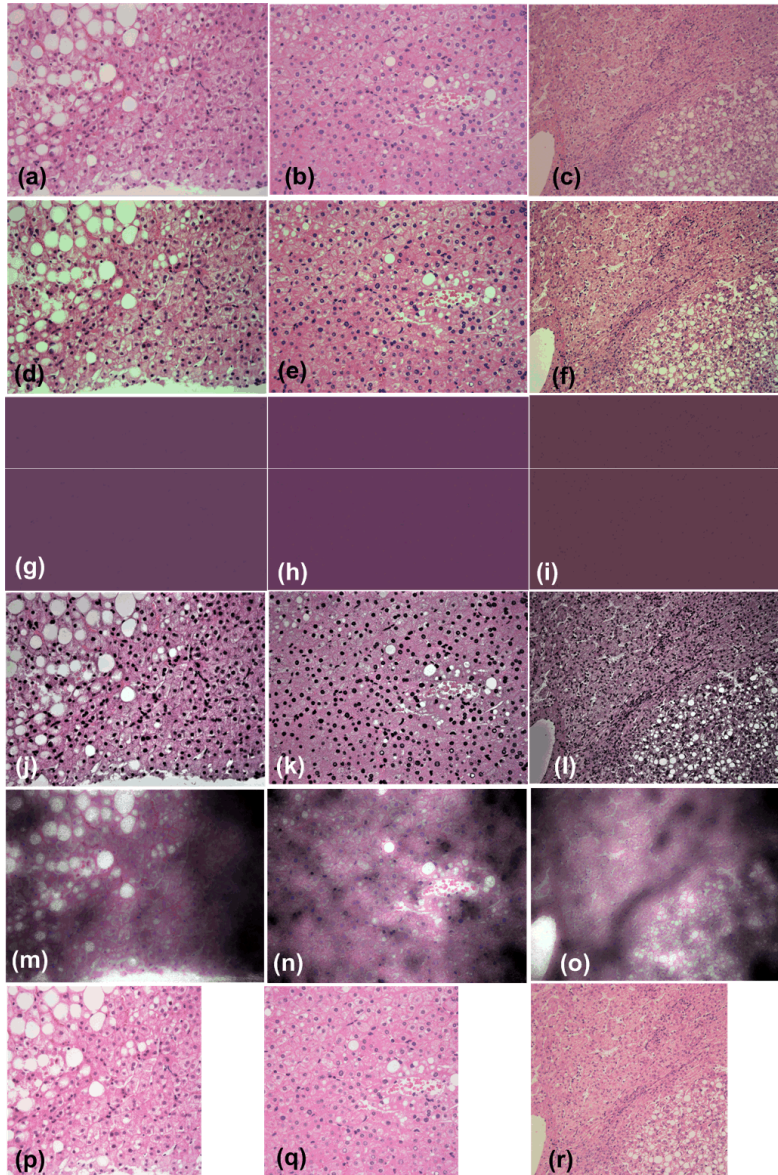


Experiments and results

The OSD image enhancement method has been evaluated comparatively on **35 specimens** of the human liver and **1 specimen of the mouse liver stained with H&E**, **6 specimens of the mouse liver stained with Sudan III**, and **3 specimens of the human liver stained with the anti-CD34 monoclonal antibody**.

Detailed diagnostic information

Stain	Human liver: Diagnosis and number of specimens	Mouse liver: Diagnosis and number of specimens
H&E Total: 36	Fatty liver: 14; hepatocellular carcinoma: 8; metastasis of colon cancer: 12; metastasis of pancreatic adenocarcinoma: 1	Fatty liver: 1
Sudan III Total: 6		Fatty liver: 6
Anti-CD34 antibody Total: 3	Fatty liver: 3	



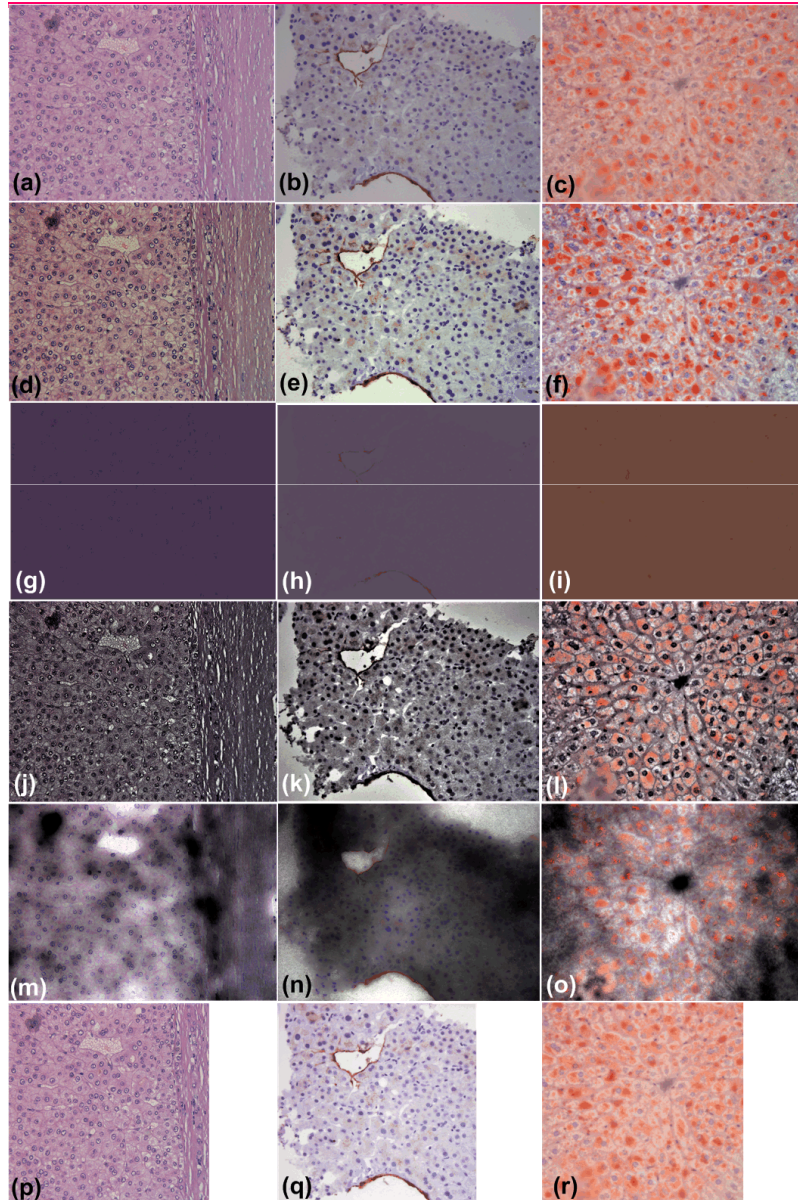
Images of the H&E-stained specimen of (a) and (b) human fatty liver; (c) hepatocellular carcinoma. (d)–(f): Images **enhanced with OSD algorithm** corresponding to stained images (a)–(c), respectively. (g)–(i): **Color offset images** obtained by **OSD algorithm** corresponding to stained images (a)–(c), respectively. (j)–(l): Images **enhanced with L^1 -Retinex algorithm** corresponding to stained images (a)–(c), respectively. (m)–(o): **Shadow images** obtained by **L^1 -Retinex algorithm** corresponding to stained images (a)–(c), respectively. (p)–(r): Images **enhanced with DWT-ST-SURE algorithm** corresponding to stained images (a)–(c), respectively.



Experiments and results

Relative values, in percentage, of quality measures for images shown previously. For each image, the best value for each measure is in bold.

	OSD			L^1 -Retinex			DWT-SURE-ST		
	(d)	(e)	(f)	(j)	(k)	(l)	(p)	(q)	(r)
Colorful	38.6	50.24	62.92	-40.57	-49.53	-30.55	11.62	10.61	-3.66
MOS	10	13.63	13.63	-20.00	-50.00	-36.36	-15.00	-13.63	-4.54
Sharpness	0.14	0.25	0.38	68.44	71.18	28.34	-21.76	-21.11	-23.60
Contrast	-9.84	-10.33	-12.43	-65.28	-39.13	-49.11	0.52	3.8	5.92



(a) Image of the H&E-stained specimen of human liver with hepatocellular carcinoma. (b) Image of anti-CD34-stained specimen of human fatty liver. (c) Image of Sudan III-stained specimen of mouse fatty liver. (d)–(f): **Images enhanced with OSD** algorithm corresponding to stained images (a)–(c), respectively. (g)–(i): **Color offset** images obtained by **OSD** algorithm corresponding to stained images (a)–(c), respectively. (j)–(l): **Images enhanced with L¹-Retinex** algorithm corresponding to stained images (a)–(c), respectively. (m)–(o): **Shadow images** obtained by **L¹-Retinex** algorithm corresponding to stained images (a)–(c), respectively. (p)–(r): Images **enhanced with DWT-ST-SURE** algorithm corresponding to stained images (a)–(c), respectively.



Experiments and results

Relative values, in percentage, of quality measures for images shown previously. For each image, the best value for each measure is in bold.

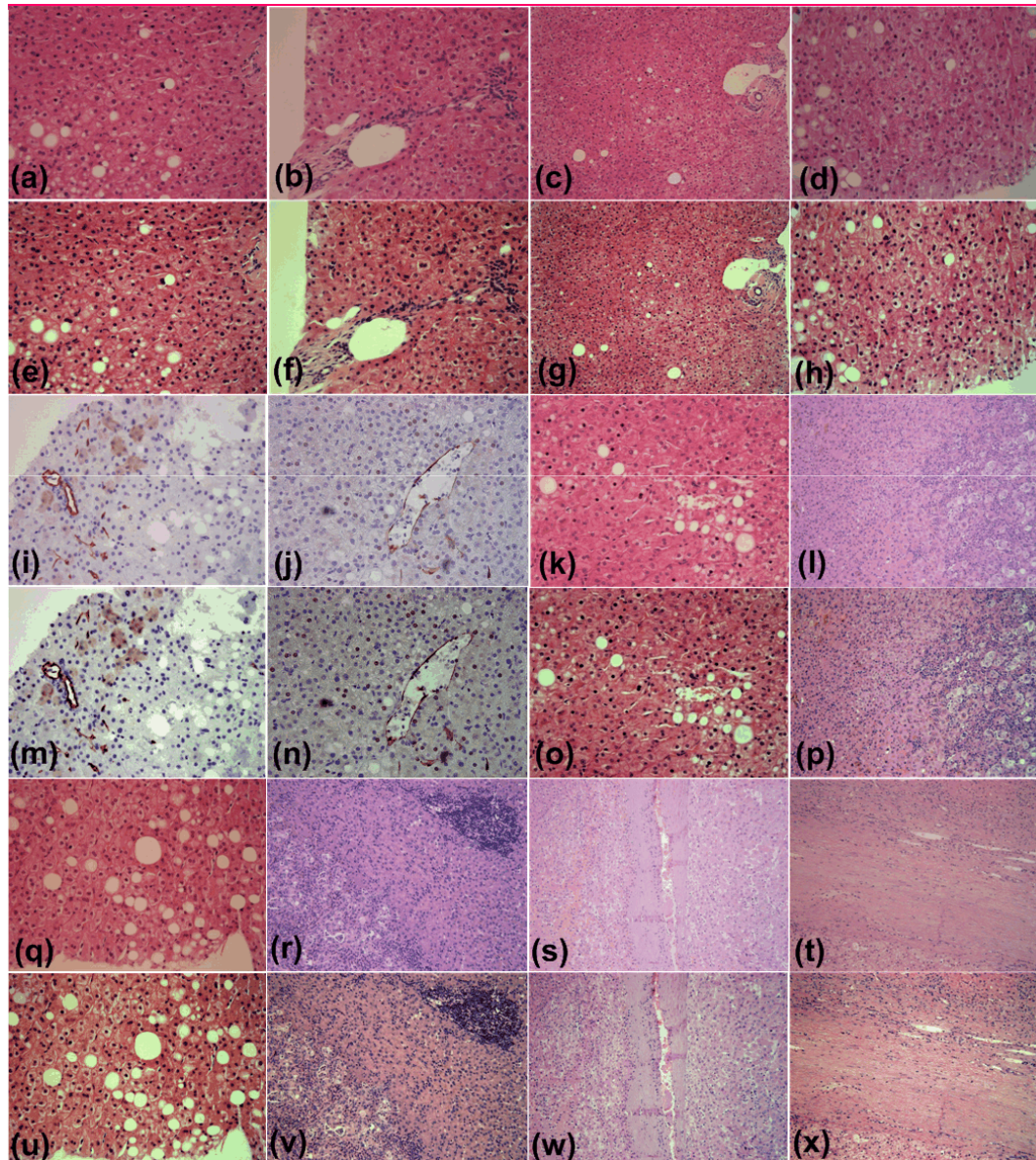
	OSD			L^1 -Retinex			DWT-SURE-ST		
	(d)	(e)	(f)	(j)	(k)	(l)	(p)	(q)	(r)
Colorful	39.51	107.47	62.47	-37.32	-39.86	19.88	5.12	38.43	6.9
MOS	25.00	15.00	56.25	-55.00	-70.00	-6.25	0.00	15.00	0.00
Sharpness	1.84	0.82	0.31	16.94	83.42	80.16	-21.55	-12.48	-29.84
Contrast	-14.1	-8.29	-8.42	-57.05	-37.07	-39.11	10.9	0	2.97



Experiments and results

Mean values and 99% confidence intervals (CI) of the estimated relative image quality measures for 45 images. The best values are in bold.

	Colorfulness		MOS		Sharpness		Contrast	
	Mean [%]	99% CI [%]	Mean [%]	99% CI [%]	Mean [%]	99% CI [%]	Mean [%]	99% CI [%]
OSD	43.86	[35.35, 51.62]	16.60	[10.46, 22.73]	1.45	[-1.97, 4.86]	-10.78	[-13.16, -8.4]
L^1 -Retinex	-26.31	[-33.67, -18.95]	-37.40	[-47.27, -27.54]	50.36	[41.59, 59.13]	-45.73	[-50.21, -41.25]
DWT-SURE-ST	6.84	[2.51, 11.17]	-3.67	[-6.62, -0.71]	-21.56	[-23.23, -19.89]	5.16	[2.61, 7.71]



(a)–(d): H&E-stained specimen of human fatty liver. **(e)–(h): OSD-enhanced** images corresponding to images of stained specimens (a)–(d), respectively.

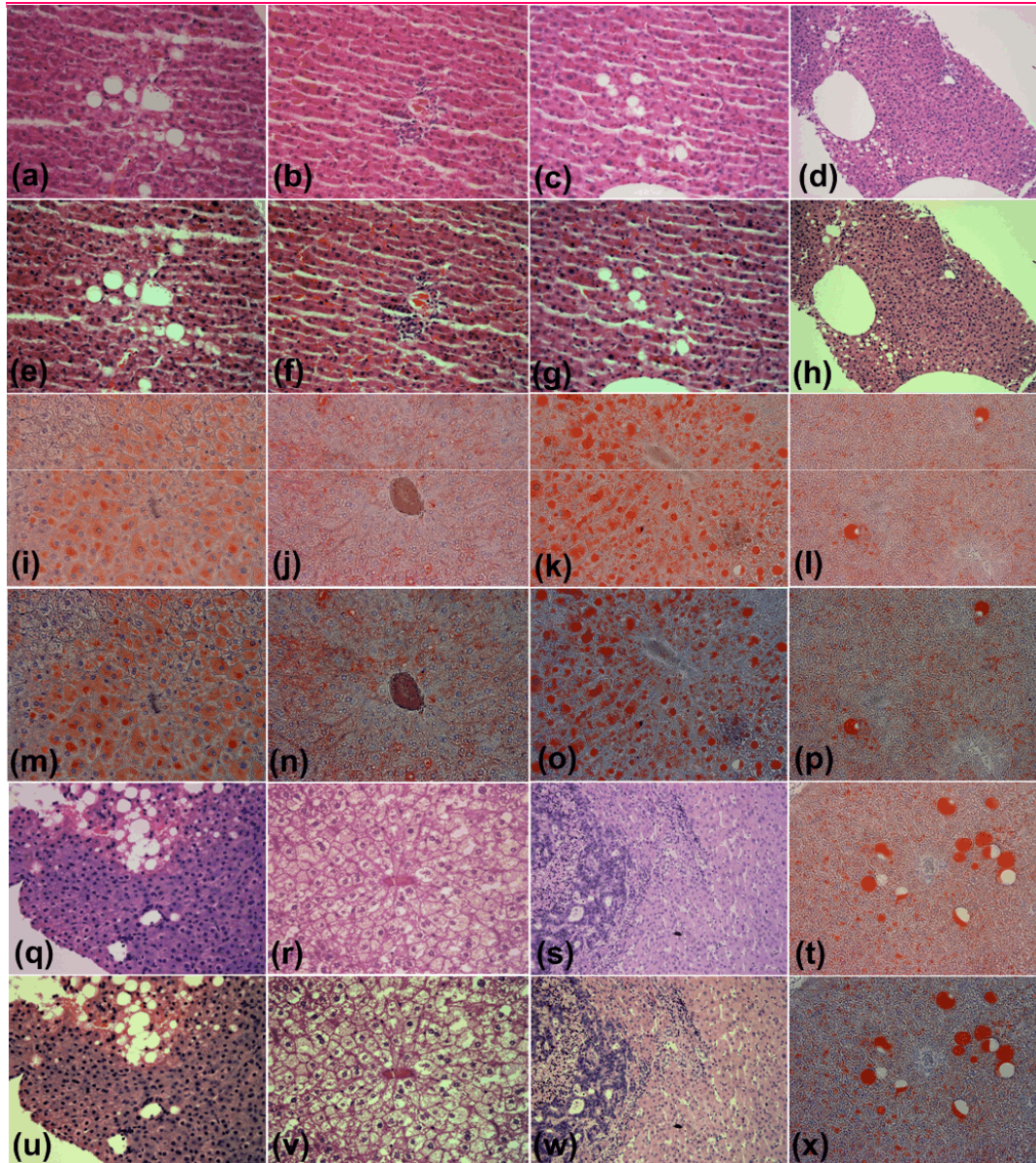
Specimens of human fatty liver: (i) and (j): anti-CD34-stained; (k) H&E-stained. (l) H&E-stained specimen of human liver with metastasis of colon cancer. **(m)–(p):**

Images enhanced with OSD algorithm corresponding to images of stained specimens (i)–(l), respectively. (q) H&E-

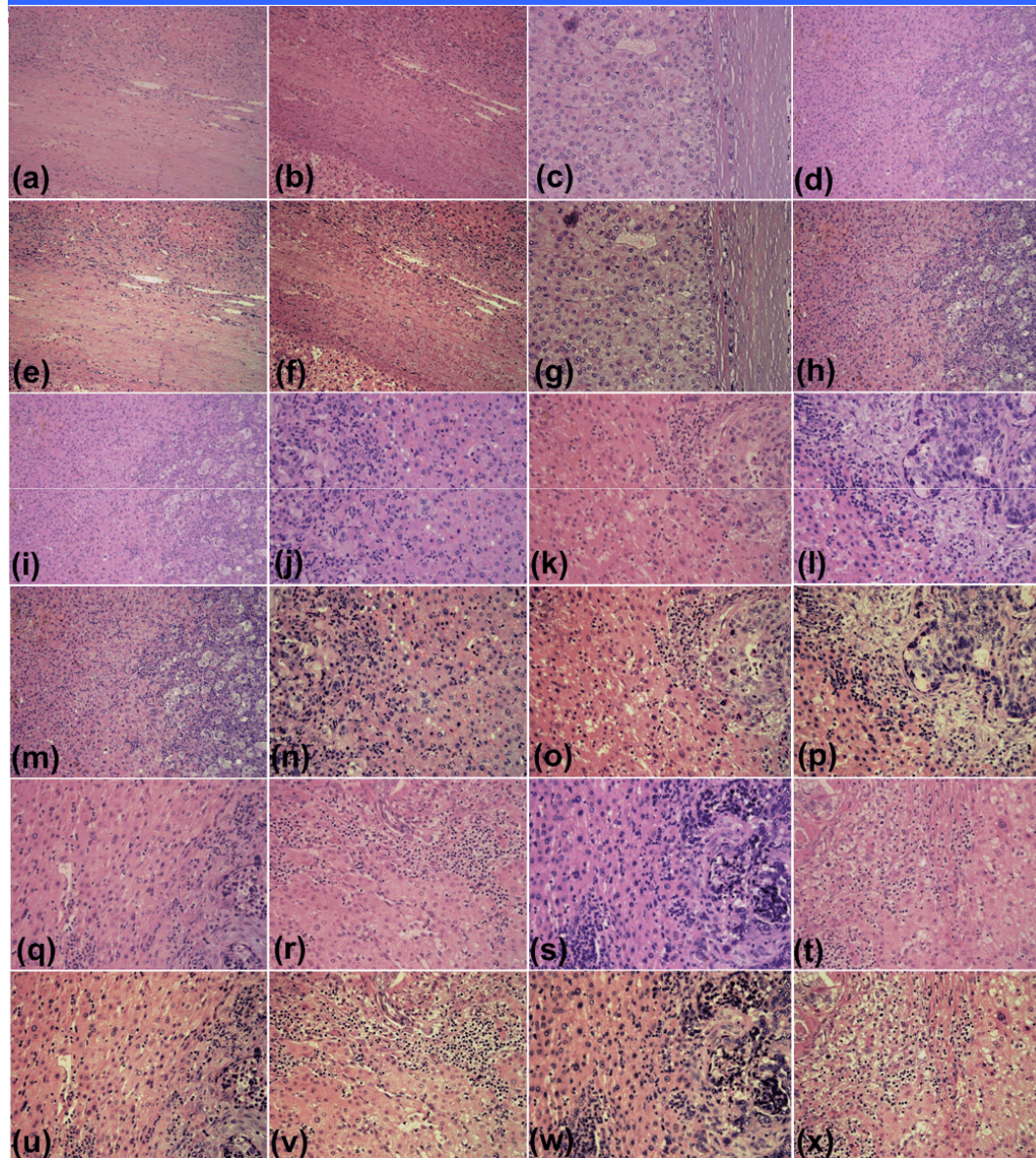
stained specimen of human fatty liver. (r) H&E-stained specimen of human liver with metastasis of gastric cancer. (s) and (t)

H&E-stained human liver with hepatocellular carcinoma. **(u)–(x): Images enhanced with OSD** algorithm

corresponding to images of stained specimens (q)–(t), respectively.



(a)–(d): H&E-stained specimen of human fatty liver. **(e)–(h): OSD-enhanced images** corresponding to images of stained specimens (a)–(d), respectively. (i)–(l): Sudan III-stained specimens of mouse fatty liver. **(m)–(p) OSD-enhanced images** corresponding to images of stained specimens (i)–(l), respectively. (q) H&E-stained specimen of human fatty liver. (r) H&E-stained specimen of mouse fatty liver. (s) H&E-stained human liver with metastasis of colon cancer. (t) Sudan III-stained specimen of mouse fatty liver. **(u)–(x): Images enhanced with OSD** algorithm corresponding to images of stained specimens (q)–(t), respectively.



(a)–(d): H&E-stained specimens of human liver with hepatocellular carcinoma. (d) H&E-stained specimen of human liver with metastasis of colon cancer. **(e)–(h): OSD-enhanced images** corresponding to images of stained specimens (a)–(d), respectively. (i)–(l): H&E-stained specimen of human liver with metastasis of colon cancer. **(m)–(p): OSD-enhanced images** corresponding to images of stained specimens (i)–(l), respectively. (q)–(t): H&E-stained specimen of human liver with metastasis of colon cancer. **(u)–(x): Images enhanced with OSD algorithm** corresponding to images of stained specimens (q)–(t), respectively.



Summary

We have developed a new method for the automated enhancement of a color microscopic image of a stained specimen in histopathology and have named it the OSD method.

This method was demonstrated on images of specimens stained with H&E, Sudan III, and anti-CD34 monoclonal antibody. The OSD method, compared to the original images of stained specimens, improved the colorimetric difference by an average of 43.86% with 99% CI of [35.35%, 51.62%].

On the basis of MOS, we concluded that the OSD-enhanced images, compared with the original images of the stained specimens, improved quality by an average of 16.60% with 99% CI of [10.46%, 22.73%].

Therefore, we conclude that the OSD method can be used to complement (assist) pathologists in looking for visual cues and in assessing a diagnosis.



Fourth Croatian Computer Vision Workshop (CCVW 2015), Faculty of Electrical Engineering and Computing, University of Zagreb,
-September 22,2015, Zagreb, Croatia

"Offset-sparsity decomposition for enhancement of microscopic images of stained specimens in histopathology"

THANK YOU !!!!!!!!